

THE CORRECTION OF CURRENT LIFTING ROTOR  
THEORY FOR THE EFFECTS OF THE RADIAL  
VELOCITY COMPONENT

A THESIS


Presented to  
the Faculty of the Graduate Division  
by

Charles R. Cunningham

In Partial Fulfillment  
of the Requirements for the Degree  
Master of Science in Aeronautical Engineering

Georgia Institute of Technology

May, 1962



"In presenting the dissertation as a partial fulfillment of the requirements for an advanced degree from the Georgia Institute of Technology, I agree that the Library of the Institution shall make it available for inspection and circulation in accordance with its regulations governing materials of this type. I agree that permission to copy from, or to publish from, this dissertation may be granted by the professor under whose direction it was written, or, in his absence, by the dean of the Graduate Division when such copying or publication is solely for scholarly purposes and does not involve potential financial gain. It is understood that any copying from, or publication of, this dissertation which involves potential financial gain will not be allowed without written permission.

---

0

30  
12R

THE CORRECTION OF CURRENT LIFTING ROTOR  
THEORY FOR THE EFFECTS OF THE RADIAL  
VELOCITY COMPONENT

Approved:

\_\_\_\_\_  
\_\_\_\_\_  
\_\_\_\_\_  
\_\_\_\_\_  
\_\_\_\_\_

Date Approved by Chairman:

May 16, 1962

## ACKNOWLEDGMENTS

The author wishes to express his sincere appreciation to Professor Walter Castles, Jr. for the suggestion of the topic and for his valuable guidance throughout the conduct of this study. Gratitude is also extended to Doctor Robin B. Gray and Doctor Thomas W. Jackson for their review and comments on the material contained herein.

## TABLE OF CONTENTS

	Page
ACKNOWLEDGMENTS .....	ii
LIST OF FIGURES .....	iv
LIST OF SYMBOLS .....	v
SUMMARY .....	x
CHAPTER	
I. INTRODUCTION .....	1
II. THEORETICAL ANALYSIS .....	3
Blade Bound Vortex Distribution	
Rotor Thrust Force	
Rotor Thrust Moment	
Rotor Rolling Moment	
Rotor Pitching Moment	
Equilibrium Solution for Rotor Parameters	
Rotor Lift Power	
Rotor Profile Power	
Total Helicopter Power Required	
III. APPLICATION .....	34
IV. CONCLUSIONS .....	36
FIGURES .....	37
APPENDIX .....	43
Equilibrium Factors	
X-Force Equation	
Power Equation	
BIBLIOGRAPHY .....	45

# LIST OF FIGURES

Figure		Page
1.	Freestream and Relative Velocity Components in Rotor Tip-Path Plane Co-ordinate System .....	37
2.	Three View of Flow Planes, Velocity Components, and Flow Angles .....	38
3.	Force Components in Plane Perpendicular to Blade Axis .....	39
4.	Blade Loading and Moment Diagram .....	40
 Table		
1.	Integral Multipliers for Various Helicopter Forward Speed Ratios .....	41
2.	Values Used in Example Problem .....	42

## LIST OF SYMBOLS

- $\alpha'$  rotor blade element angle of attack in true flow plane  
 $\alpha_R$  rotor angle of attack (positive below TPP and  $\approx \tan^{-1} D_F/W$ )  
 $\delta_o$  constant part of profile drag coefficient ( $\approx 0.008$ )  
 $\epsilon$  variable part of profile drag coefficient ( $\approx 0.008$ )  
 $\Gamma$  local blade circulation  
 $\lambda$  non-dimensional component of velocity perpendicular to TPP ,  

$$\lambda = \frac{V \sin \alpha_R - v}{\Omega R}$$
  
 $\eta$  angle between true flow plane and plane perpendicular to blade axis  
 $\mu$  helicopter advance ratio or forward speed ratio,  $\mu = \frac{V \cos \alpha_R}{\Omega R}$   
 $\Omega$  rotor angular velocity  
 $\bar{\alpha}_n$  integral multiplier in equation for lift power coefficient,  

$$\bar{\alpha}_n = \int_{x_1}^{x_2} \frac{x^{n-1} dx}{(x^2 + \mu^2)^{3/2}}$$
  
 $\bar{\alpha}'_n$  integral multiplier in equation for profile power coefficient,  

$$\bar{\alpha}'_n = \int_{x_1}^{x_2} \frac{x^{n-1} dx}{[x^2 + (\mu^2 + \lambda^2)]^{3/2}}$$
  
 $\rho$  air density  
 $\phi$  inflow angle in plane perpendicular to blade axis  
 $\phi'$  inflow angle in true flow plane  
 $\psi$  blade angular or azimuth position

- $\sigma$  rotor solidity,  $\sigma = bc/\pi R$
- $\theta$  blade element angle in plane perpendicular to blade axis,  $\theta = A_0 + \theta_1 x - a_1 \sin \psi + b_1 \cos \psi$
- $\theta_1$  blade twist (negative for washout)
- $\theta'$  blade element angle in true flow plane
- $a_0$  rotor coning angle
- $A_0$  rotor collective pitch used to control thrust, rotor rpm, normal acceleration, etc.
- $a_1$  rotor blade lateral cyclic pitch (furnishes normal acceleration control at high speed)
- $a$  slope of blade element lift curve ( $\approx 2\pi$ )
- $b_1$  rotor blade longitudinal cyclic pitch (furnished bank angle control)
- $b$  number of blades in rotor
- $c'$  blade chord in true flow plane
- $c$  blade chord in plane perpendicular to blade axis
- $C_{do}$  local blade element profile drag coefficient,  $C_{do} = 2 C_f (1 + C_l^2)$
- $C_f$  skin friction drag coefficient ( $\approx 0.004$ )
- $C_l$  local blade element lift coefficient
- $C_{in}$  coefficient in box of the i-th column and the n-th row of power coefficient equations
- $C_{MT}$  non-dimensional average blade thrust moment coefficient,  

$$C_{MT} = \frac{M_T}{\rho \pi \Omega^2 R^5}$$
- $C_{MX}$  non-dimensional rotor rolling moment coefficient,  $C_{MX} = \frac{M_X}{\rho \pi \Omega^2 R^5}$
- $C_{MY}$  non-dimensional rotor pitching moment coefficient,  $C_{MY} = \frac{M_Y}{\rho \pi \Omega^2 R^5}$
- $C_P$  power coefficient,  $C_P = \frac{P}{\rho \pi \Omega^3 R^5}$
- $C_{PR}$  helicopter power coefficient neglecting radial component of velocity



- $C_{PRL}$  lift power coefficient with radial component  
 $C_{PRD}$  profile power coefficient with radial component  
 $C_{PRT}$  helicopter power coefficient with radial component,  $C_{PRT} = C_{PRL} + C_{PRD}$   
 $C_T$  average rotor thrust coefficient,  $C_T = \frac{T}{\rho \pi \Omega^2 R^4}$   
 $C'_T$  rotor blade thrust force coefficient  
 $C_X$  rotor X force coefficient,  $C_X = F_X / \frac{1}{2} \rho \pi \Omega^2 R^4$   
 $dD$  represents the resultant blade element differential profile drag force  
 $(dD)_a$  axial component of differential blade element profile drag force  
 $(dD)_r$  radial component of differential blade element profile drag force  
 $(dD)_t$  tangential component of differential blade element profile drag force  
 $D_F$  fuselage parasite drag force,  $D_F = f \frac{1}{2} \rho v^2$   
 $F$  variable term in binomial expansion,  $F = \frac{\mu x \sin \psi}{x^2 + \mu^2}$   
 $F_X$  rotor X-force  
 $f$  fuselage equivalent parasite area  
 $G$  variable term in binomial expansion,  $G \approx \frac{\mu x \sin \psi}{x^2 + \mu^2 + \lambda^2}$   
 $I_1$  rotor blade mass moment of inertia  
 $K$  rotor blade inertia factor,  $K = \frac{\rho \pi R^5 \sigma a}{2bI_1}$   
 $dL$  represents the blade element resultant differential lift force  
 $(dL)_a$  axial component of differential blade element lift force  
 $(dL)_t$  tangential component of differential blade element lift force  
 $M$  equilibrium factor, term in  $a_1$  or  $A_0$  equation (see Appendix)  
 $M_T$  rotor blade thrust moment  
 $M_X$  rotor rolling moment  
 $M_Y$  rotor pitching moment  
 $N$  equilibrium factor, term in  $a_1$  or  $A_0$  equation (see Appendix)

- P power
- $P_R$  total rotor shaft horsepower required,  $P_R = (C_{PRL} + C_{PRD}) \rho \pi \Omega^3 R^5 / 550$   
or  $P_R = C_{PR} \rho \pi \Omega^3 R^5 / 550$
- r radial position on rotor blade in TPP
- R blade radius
- S equilibrium factor, term in  $a_1$  or  $A_0$  equation (see Appendix)
- T rotor thrust force
- dT differential blade element rotor thrust force,  $dT \quad (dL)_a$
- TPP abbreviation for tip-path plane
- U resultant blade element velocity,  $U = \Omega R \sqrt{v_a^2 + v_t^2 + v_r^2}$
- V flight path velocity
- v uniform induced velocity,  $v = \frac{\frac{1}{2} C_T \Omega R}{(\lambda^2 + \mu^2)^{1/2}}$
- $V_A$  freestream inflow velocity ratio,  $V_A = \frac{V \sin \alpha_R}{\Omega R}$
- $v_i$  triangular induced velocity distribution, non-dimensional coefficient  
$$v_i = \frac{\frac{3}{4} C_T}{(1 - \mu^2) \sqrt{(V_A - \frac{3}{4} v_i)^2 + \mu^2}}$$
- $v_a$  non-dimensional axial component of resultant blade element velocity,  $v_a = \lambda - a_0 \mu \cos \psi$
- $v_r$  non-dimensional radial component of resultant blade element velocity,  $v_r = \mu \cos \psi$
- $v_t$  non-dimensional tangential component of resultant blade element velocity,  $v_t = x + \mu \sin \psi$
- W helicopter weight
- x non-dimensional rotor blade radius,  $x = r/R$
- $x_1$  non-dimensional inboard blade section radius,  $x_1 = r_1/R$
- $x_2$  non-dimensional effective outboard blade section radius,  $x_2 = r_2/R$
- X,Y,Z equilibrium factors, terms in  $a_1$  or  $A_0$  equation (see Appendix), also tip-path plane axes designations

ZLL abbreviation for blade element zero lift chord line

$\Omega R$  rotor blade rotational tip speed

## SUMMARY

As the forward speed ratios of helicopters increase, it becomes necessary at some point to take into account the radial velocity corrections. The purpose of this study is to correct current lifting rotor theory for the effects of the radial component of resultant blade element velocity.

Force, moment, and power equations, including the effects of the radial component of the resultant velocity at the rotor blade elements, are derived. Since certain integral multipliers appear repeatedly in all equations derived, these multipliers were evaluated for flight conditions ranging from forward speed ratios of zero to one. The results of the evaluations of the integral multipliers are presented in tabular form in order to facilitate computations involved in applying the derived equations. Values in the tabular form were determined utilizing a Burroughs 220 computer.

The derived equations are set up with the assumptions of uniform induced velocity distribution. Second and higher harmonic flapping is neglected. Tip-path plane co-ordinates are used. Further, the assumption of constant chord blades is made throughout. The effects of linear blade twist are included in the equations.

A theoretical comparison is made between results obtained, using the equations derived herein and similar equations which neglect the effects of the radial component. The comparison was made for a current production-model helicopter. The comparison shows that, at a forward

speed of 193 mph, the calculated total power required increases approximately 15 per cent when the effects of the radial velocity component at the blade elements are taken into account.

Moreover, it was found that both the rotor lift and profile powers increased due to the radial velocity component. Of the two, the per cent increase in the profile power is greater.



## CHAPTER I

### INTRODUCTION

The majority of current helicopters are designed to fly at top forward speeds which range from 100 to 150 mph, although speeds as high as 200 mph have been obtained. Contemporary lifting rotor theory, such as that used in performance prediction, gives results that agree reasonably well with flight test data for the speed range mentioned above.

However, the mathematical labor involved in developing contemporary lifting rotor theory is considerable, and to simplify this mathematical complexity most authors have disregarded the effects of the radial component of freestream velocity acting at the blade elements (as seen in Fig. 1).

With the advent of helicopter designs which have projected flight speeds well above present ranges, the contemporary theories that neglect the effects of the radial component may become inadequate. In particular, it is believed that contemporary performance theory, taking into account only the tangential and axial components of the resultant velocity at the blade elements, will underestimate the helicopter power required, the error becoming greater at higher forward speeds.

The purpose of this paper is to correct contemporary lifting rotor theory by including the effects of the radial component. This will be done by employing certain series expansions for the blade bound vortex strength and the resultant velocity at the blade elements, as described in Reference 1.

In general, the basic assumptions of two-dimensional airfoil theory will be adhered to throughout. Compressibility will not be considered, except in the effect on the average blade element lift curve slope. Equations derived will automatically take into account the reversed flow region, and be applicable for large inflow angles. As stated earlier, applications will be made to constant chord, linearly twisted blades only.

It is the aim of this study to gain a general idea of the error involved in contemporary theory which neglects the radial component. To do this, a typical problem will be considered. Using the derived power-required equation and a similar relation from Reference 2 which neglects the radial component, the difference in the power required at a given flight condition will be computed.

## CHAPTER II

### THEORETICAL ANALYSIS

Blade Bound Vortex Distribution.--A typical rotor tip-path plane coordinate system is chosen, as shown in Fig. 1. The tip-path plane can be visualized as that plane described by the blade tips of an operating helicopter main-rotor system. The z-axis is perpendicular to the tip-path plane in the direction of the thrust. The x- and y-axes lie fixed in the tip-path plane with the x-axis directed downwind and the y-axis directed to starboard. Let the flight path or freestream velocity be  $V$  and the rotor angle of attack be  $\alpha_R$ .

As is usually assumed for simplicity in making approximate rotor performance calculations, let the induced velocity,  $v$ , be uniform over the rotor disk area swept by the blades. Also, neglect second and higher harmonic rotor flapping motions, since these effects are small in most applications.

A rotating system of helicopter rotor blades describes a cone as a result of mass centrifugal forces balancing blade aerodynamic forces in the flapping mode. With respect to the tip-path plane, the described cone is of base angle,  $a_0$ , called the coning angle in helicopter terminology. The coning angle will be assumed small so that  $\sin a_0 \approx a_0$  and the  $\cos a_0 \approx 1$ .

For simplicity, assume the  $b$  number of blades in the main rotor are of constant chord,  $c$ . Let the rotor angular velocity be  $\Omega$  and the rotor blade radius be  $R$ . Then the relative velocity components



acting along the blade at any radial position,  $r$ , become

$$(\text{axial component}) = V \sin \alpha_R - v - (V \cos \alpha_R \cos \psi) a_o \quad (1)$$

$$(\text{tangential component}) = \Omega r + V \cos \alpha_R \sin \psi \quad (2)$$

$$(\text{radial component}) = V \cos \alpha_R \cos \psi \quad (3)$$

where, as assumed previously,  $a_o$  is small and  $\psi$  is the blade azimuth position measured from the downwind x-axis in the direction of rotation, as shown in Fig. 1.

In non-dimensional form, which will be convenient for subsequent derivations, Equations (1), (2), and (3) become

$$(\text{axial component}) v_a = \lambda - a_o \mu \cos \psi \quad (4)$$

$$(\text{tangential component}) v_t = x + \mu \sin \psi \quad (5)$$

$$(\text{radial component}) v_r = \mu \cos \psi \quad (6)$$

where

$$\lambda = \frac{V \sin \alpha_R - v}{\Omega R}$$

$$x = \frac{r}{R}$$

$$\mu = \frac{V \cos \alpha_R}{\Omega R}$$

As shown in Fig. 2a, the blade angle measured about the blade axis and between the zero lift chord line and the tip-path plane is denoted by

$\theta$  (positive above the tip-path plane). The blade angle,  $\theta$ , is measured with respect to a blade element perpendicular to the blade axis. Let the variation in  $\theta$  for any flight condition be represented by the trigonometric series

$$\theta = A_0 + \theta_1 x - a_1 \sin \psi + b_1 \cos \psi \quad (7)$$

where the term  $\theta_1 x$  gives the blade linear twist; the term  $A_0$  represents a mean value of  $\theta$  per revolution at the blade root position; and rotor blade cyclic or feathering first harmonic motions are represented by  $-a_1 \sin \psi + b_1 \cos \psi$ .

However, from Fig. 2b it is seen that  $\theta$  is the blade angle of a blade element perpendicular to the blade feathering axis, but at an angle  $\eta$  with respect to the true flow plane. The resultant velocity at the blade element in the true flow plane is

$$U = \Omega R \sqrt{v_a^2 + v_t^2 + v_r^2} \quad (8)$$

where the rotor blade tip speed,  $\Omega R$ , dimensionalizes the terms under the radical. Equation (8) gives the resultant velocity acting on a yawed blade section of chord  $c'$  shown in Fig. 2c. Thus, the Kutta condition at the blade trailing edge (assumed sharp) which determines the blade circulation or bound vortex strength, is actually satisfied in the true flow plane of Fig. 2c. It is significant to point out that contemporary theory, neglecting  $v_r$ , assumes the Kutta condition to be satisfied in the plane perpendicular to the blade axis shown in Fig. 2a.

In the present case where part of the flow is "frozen" to the blade

on account of the rotation of the co-ordinate system, the usual two-dimensional skewed flow approximations do not apply. For example, if the blade axis were warped to that three-dimensional curved shape which would give the same angle of attack and skew angle distribution in a rectilinear flow as the actual blade experiences in the real flow, then the bound and wake vortex configurations would be entirely different.

Hence, working in the true flow plane in which the Kutta condition is satisfied, let the true blade angle be  $\theta'$ . Then, as deduced from the geometry of Fig. 2b

$$\theta' = \theta \cos \eta = \theta \frac{v_t}{\sqrt{v_t^2 + v_r^2}} \quad (9)$$

Likewise, from Fig. 2c the true inflow angle,  $\phi'$ , measured between the tip-path plane and the rotor blade resultant velocity,  $U$ , is

$$\phi' = \tan^{-1} \frac{v_a}{\sqrt{v_t^2 + v_r^2}} \quad (10)$$

The yawed blade chord,  $c'$ , is seen from Fig. 2b to be

$$c' = c \sec \eta = c \frac{\sqrt{v_t^2 + v_r^2}}{v_t} \quad (11)$$

where  $c$  is of constant magnitude and  $c'$  changes with  $\psi$ . Note that  $c'$  is measured in the true flow plane or parallel to  $U$ .

Let the true angle of attack be denoted by  $\alpha'$  and measured between the zero lift line and  $U$  in Fig. 2c. The true angle of attack

which determines the blade circulation is then

$$\alpha' = \theta' + \phi' \quad (12)$$

Two-dimensional airfoil theory demonstrates from Reference 3 that for local blade element lift coefficients up to the stall

$$\frac{C_l}{a} = \sin \alpha' = \sin(\theta' + \phi') \quad (13)$$

where  $a$  = slope of lift curve. For the helicopter blade airfoil for which  $\theta'$  is a small angle (although the inflow angle  $\phi'$  is not necessarily small) it follows that  $\sin \theta' \approx \theta'$  and  $\cos \theta' \approx 1$ . Hence, upon expanding Equation (13) with the trigonometric formula for the sine of the sum of two angles the result is

$$\frac{C_l}{a} = \theta' \cos \phi' + \sin \phi' \quad (14)$$

The local blade circulation,  $\Gamma$ , of a blade element in the true flow plane at position  $(x, \psi)$  is deduced from theoretical and experimental aerodynamic expressions for the lift force acting perpendicular to  $U$  and given by

$$\Gamma = \frac{1}{2} c' C_l U \quad (15)$$

Finally, the expression for the rotor blade bound vortex strength about a blade section in the true flow plane at any position  $(x, \psi)$  of the tip-path plane is found by substituting Equations (8), (9), (10), (11), and (14) into Equation (15). After simple algebraic manipulations,

the result is

$$\frac{2\Gamma}{ac\Omega R} = \left(\theta + \frac{v_a}{v_t}\right) \sqrt{v_t^2 + v_r^2} \quad (16)$$

The significance of Equation (16) is twofold. First, it includes the effects of  $v_r$  which will enable the effects of the radial component to be introduced into subsequent force and power expressions. Second,  $\Gamma$  retains the correct sign in the reversed flow region (i.e., positive with respect to a negative  $U$ ), and thus affords continuous load distributions for vibration analyses and obviates the necessity of making reverse flow corrections.

Rotor Thrust Force.--In this section an equation including the effects of  $v_r$  and representing the mean rotor thrust force per revolution will be derived. The differential lift force,  $dL$ , acting on the differential blade element,  $cdr$ , located in the tip-path plane at position  $(r, \psi)$  is obtained as

$$dL = \rho \Omega R \Gamma \sqrt{v_a^2 + v_t^2} dr \quad (17)$$

which is shown in Fig. 3. The tip speed,  $\Omega R$ , is included in Equation (17) to dimensionalize the terms under the radical.

The resultant differential lift force can be broken into a differential axial force component,  $(dL)_a$ , perpendicular to the tip-path plane, and into the tangential component,  $(dL)_t$ , parallel to the tip-path plane. With reference to Fig. 3, the axial component can be found by resolving  $dL$  into the axial direction. Thus, from similar triangles, Equation (17)



is multiplied by  $\cos \phi = v_t / \sqrt{v_a^2 + v_t^2}$  resulting in

$$(dL)_a = \rho \Omega R \Gamma v_t dr \quad (18)$$

which is positive in the plus z-direction. Likewise, the tangential component is obtained by multiplying Equation (17) by  $\sin \phi = v_a / \sqrt{v_a^2 + v_t^2}$  resulting in

$$(dL)_t = - \rho \Omega R \Gamma v_a dr \quad (19)$$

assumed positive opposite the direction of rotation.

It is important to note that Equations (17), (18), and (19) have been derived with respect to the rotor normal and tangential directions. Such a treatment simplifies the derivations and does not leave out  $v_r$  since the radial component enters the equations by way of the term,  $\Gamma$ , given by Equation (16).

It should be remembered that the mean or steady value of the resultant rotor thrust force is defined as perpendicular to the tip-path plane. Then, since  $a_0$  has been assumed small, the differential axial blade force,  $(dL)_a$ , lies in the same direction as  $dT$ , the differential blade thrust force. Thus

$$(dL)_a = dT \quad (20)$$

Then from Equation (18)

$$dT = \rho \Omega R \Gamma v_t dr \quad (21)$$

Substituting Equation (16) into (21) gives

$$dT = \frac{\rho a c \Omega^2 R^2}{2} (\theta v_t + v_a) \sqrt{v_t^2 + v_r^2} dr \quad (22)$$

Define a non-dimensional blade force or thrust coefficient as

$$C_T = \frac{T}{\rho \pi \Omega^2 R^4} \quad (23)$$

and note that the differential of the non-dimensional blade radius,  $x = r/R$ , is  $\frac{dr}{R} = dx$ . Thus, Equation (22) can be re-written as

$$\frac{dC_T}{dx} = \frac{ac}{2\pi R} (\theta v_t + v_a) \sqrt{v_t^2 + v_r^2} \quad (24)$$

which gives the slope of the non-dimensional thrust loading along a blade at some azimuth position  $\psi$  (see Fig. 4). Note that  $v_r$  is included in Equation (24).

It is desired to obtain an expression for the average or mean rotor thrust force per revolution for any flight condition. The individual blade thrust is found by integrating Equation (24) from an inboard section,  $x_1$ , to some effective outboard section,  $x_2$ , near or at the tip. Then the average of the blade thrust for the revolution is found by integrating azimuthally from  $\psi = 0$  to  $\psi = 2\pi$  and dividing by  $2\pi$ . Multiplying the above by the  $b$  number of blades in the rotor system gives the desired result. Thus

$$C_T = b \left( \frac{1}{2\pi} \right) \int_0^{2\pi} \left[ \int_{x_1}^{x_2} \frac{dC_T}{dx} dx \right] d\psi \quad (25)$$

or

$$C_T = \frac{\sigma}{2} \left( \frac{1}{2\pi} \right) \int_0^{2\pi} \int_{x_1}^{x_2} \left[ (\Theta v_t + v_a) \sqrt{v_t^2 + v_r^2} \right] dx d\psi \quad (26)$$

where  $\sigma = bc/\pi R$  defined as the non-dimensional rotor solidity ratio

$x_1$  non-dimensional inboard blade limit

$x_2$  non-dimensional outboard blade limit

$$C'_T = \int_{x_1}^{x_2} \frac{dC_T}{dx} dx \quad \text{rotor blade thrust force coefficient}$$

Although Equation (26) can be readily integrated with respect to the blade radius, the result cannot, in general, be integrated in closed form with respect to blade azimuthally position  $\psi$ . However, the troublesome radical  $\sqrt{v_t^2 + v_r^2}$  can be expanded in a converging series.

Substituting Equations (5) and (6) into  $\sqrt{v_t^2 + v_r^2}$  and factoring out the average value for the revolution gives

$$\sqrt{v_t^2 + v_r^2} = \sqrt{x^2 + \mu^2} \sqrt{1 + 2F} \quad (27)$$

where

$$F = \frac{\mu x \sin \psi}{x^2 + \mu^2} \quad (28)$$

Applying the binomial expansion to the factor  $\sqrt{1 + 2F}$  on the right side of Equation (27) gives



$$\sqrt{1 + 2F} = 1 + F - \frac{1}{2} F^2 + \dots \quad (29)$$

which Castles, in Reference 1, has shown to converge for all  $\mu$ ,  $x$  and  $\psi$ , except at the isolated point  $x = \mu$  and  $\psi = 270^\circ$  where the dynamic pressure and lift force are essentially zero. Castles has also shown that utilizing only the three terms in the series gives accurate results in the calculation of blade loadings, as compared to exact numerical integration. Thus, substituting Equations (27) and (29) into (24) gives

$$\frac{dC_T}{dx} = \frac{ac}{2\pi R} (\theta v_t + v_a)(x^2 + u^2)^{1/2} (1 + F - \frac{1}{2} F^2) \quad (30)$$

At this point, it is convenient to consider the equation for the thrust force acting on a blade in position  $\psi$ . Thus, substituting Equations (28) and (30) into (25) and integrating with respect to  $x$  only gives

$$\begin{aligned} C'_T = \frac{a\sigma}{2b} \left\{ \left[ \left( \lambda \mu^4 - \frac{1}{2} a_1 \mu^5 \right) \bar{a}_1 + \left( \frac{3}{2} A_0 \mu^4 + \frac{3}{16} a_1 \mu^3 - \frac{1}{4} \lambda \mu^2 \right) \bar{a}_2 \right. \right. \\ + \left( 2 \lambda \mu^2 - \frac{3}{2} a_1 \mu^3 + \frac{3}{2} \theta_1 \mu^4 - \frac{1}{4} A_0 \mu^2 \right) \bar{a}_3 + \left( \frac{5}{2} A_0 \mu^2 - \frac{1}{4} \theta_1 \mu^2 \right) \bar{a}_4 \\ + \left( \lambda + \frac{5}{2} \theta_1 \mu^2 - a_1 \mu \right) \bar{a}_5 + (A_0) \bar{a}_6 + (\theta_1) \bar{a}_7 \Big] + \sin \psi \left[ (A_0 \mu^5) \bar{a}_1 \right. \\ + (\theta_1 \mu^5 + \lambda \mu^3 - \frac{3}{8} A_0 \mu^3 - \frac{7}{4} a_1 \mu^4) \bar{a}_2 + (3A_0 \mu^3 + \frac{3}{8} a_1 \mu^2 \\ - \frac{3}{8} \theta_1 \mu^3) \bar{a}_3 + \left( \lambda \mu + 3 \theta_1 \mu^3 - \frac{11}{4} a_1 \mu^2 \right) \bar{a}_4 + (2A_0 \mu) \bar{a}_5 + (2 \theta_1 \mu \\ - a_1) \bar{a}_6 \Big] + \cos \psi \left[ (-a_0 \mu^5) \bar{a}_1 + \left( \frac{5}{4} b_1 \mu^4 + \frac{1}{8} a_0 \mu^3 \right) \bar{a}_2 + (-2a_0 \mu^3 \right. \end{aligned}$$

$$\begin{aligned}
& - \frac{1}{8} b_1 \mu^2 \bar{\delta}_3 + \left( \frac{9}{4} b_1 \mu^2 \bar{\delta}_4 + \left( \frac{9}{4} a_0 u \right) \bar{\delta}_4 + (- a_0 \mu) \bar{\delta}_5 + (b_1) \bar{\delta}_6 \right] \\
& + \sin 2\psi \left[ \left( \frac{1}{2} b_1 \mu^5 \right) \bar{\delta}_1 + \left( - \frac{1}{2} a_0 \mu^4 - \frac{1}{8} b_1 \mu^3 \right) \bar{\delta}_2 + \left( \frac{3}{2} b_1 \mu^3 \right) \bar{\delta}_3 \right. \\
& + \left. \left( - \frac{1}{2} a_0 \mu^2 \right) \bar{\delta}_4 + (b_1 \mu) \bar{\delta}_5 \right] + \cos 2\psi \left[ \left( \frac{1}{2} a_1 \mu^5 \right) \bar{\delta}_1 + \left( - \frac{1}{2} A_0 \mu^4 \right. \right. \\
& - \frac{1}{4} a_1 \mu^3 + \frac{1}{4} \lambda \mu^2 \bar{\delta}_2 + \left. \left( \frac{3}{2} a_1 \mu^3 - \frac{1}{2} \theta_1 \mu^4 + \frac{1}{4} A_0 \mu^2 \right) \bar{\delta}_3 \right. \\
& + \left. \left( - \frac{1}{2} A_0 \mu^2 + \frac{1}{4} \theta_1 \mu^2 \right) \bar{\delta}_4 + \left( a_1 \mu - \frac{1}{2} \theta_1 \mu^2 \right) \bar{\delta}_5 \right] + \sin 3\psi \left[ \left( \frac{1}{4} a_1 \mu^4 \right. \right. \\
& + \frac{1}{8} A_0 \mu^3 \bar{\delta}_2 + \left. \left( - \frac{1}{8} a_1 \mu^2 + \frac{1}{8} \theta_1 \mu^3 \right) \bar{\delta}_3 + \left( \frac{1}{4} a_1 \mu^2 \right) \bar{\delta}_4 \right] \\
& + \cos 3\psi \left[ \left( - \frac{1}{4} b_1 \mu^4 - \frac{1}{8} a_0 \mu^3 \right) \bar{\delta}_2 + \left( \frac{1}{8} b_1 \mu^2 \right) \bar{\delta}_3 + \left( - \frac{1}{4} b_1 \mu^2 \right) \bar{\delta}_4 \right] \\
& + \sin 4\psi \left[ \left( \frac{1}{16} b_1 \mu^3 \right) \bar{\delta}_2 \right] + \cos 4\psi \left[ \left( \frac{1}{16} a_1 \mu^3 \right) \bar{\delta}_2 \right] \quad (31)
\end{aligned}$$

where the multipliers  $\bar{\delta}_n = 1, 2, 3, 4, \dots$  are representative of the general integral

$$\bar{\delta}_n = \int_{x_1}^{x_2} \frac{x^{n-1} dx}{(x^2 + \mu^2)^{3/2}} \quad (32)$$

Substituting Equation (31) into (25) and integrating with respect to  $\psi$  gives the mean or average value of the non-dimensional rotor thrust force

per revolution as

$$\begin{aligned}
 C_T = \frac{a\sigma}{2} & \left[ (\lambda \mu^4 - \frac{1}{2} a_1 \mu^5) \bar{\Phi}_1 + (\frac{3}{2} A_0 \mu^4 + \frac{3}{16} a_1 \mu^3 - \frac{1}{4} \lambda \mu^2) \bar{\Phi}_2 \right. \\
 & + (2 \lambda \mu^2 - \frac{3}{2} a_1 \mu^3 + \frac{3}{2} \theta_1 \mu^4 - \frac{1}{4} A_0 \mu^2) \bar{\Phi}_3 + (\frac{5}{2} A_0 \mu^2 - \frac{1}{4} \theta_1 \mu^2) \bar{\Phi}_4 \\
 & \left. + (\lambda + \frac{5}{2} \theta_1 \mu^2 - a_1 \mu) \bar{\Phi}_5 + (A_0) \bar{\Phi}_6 + (\theta_1) \bar{\Phi}_7 \right] \quad (33)
 \end{aligned}$$

The use of Equations (31) and (33) is facilitated since the integral multipliers,  $\bar{\Phi}_n = 1, 2, 3, \dots$  are tabulated for various values of forward speed ratio,  $\mu$ , in Table I. To use Table I for values of  $\mu$  falling between those given, conventional interpolation techniques should be used. The unknowns  $a_0$ ,  $A_0$ ,  $a_1$  and  $b_1$  can be evaluated from expressions which will be developed in subsequent sections.

It is important to note that a simplification was afforded in obtaining Equation (33) by integrating Equation (31) with respect to  $\psi$ . Note that such terms as  $\sin m \psi$  or  $\cos m \psi$  reduce to zero when integrated as

$$\int_0^{2\pi} (\sin m \psi \text{ or } \cos m \psi) d\psi = 0 \quad (34)$$

where  $m = 1, 2, 3, 4, \dots$

Rotor Thrust Moment.--In this section an equation including the effects of  $v_r$  and representing the mean rotor thrust moment will be derived. Consider a rotor blade at some azimuth position,  $\psi$ , as shown in Fig. 4. Distributed along the span of this blade from  $x_1$  to  $x_2$  and acting in the

axial or positive z-direction is the varying aerodynamic force or thrust distribution (called the thrust loading), given by Equation (30).

Considering only the instantaneous thrust loading on the blade in position  $\psi$ , it is seen that the unbalanced force distribution will produce a moment about the blade root called the rotor blade thrust moment,  $M_T$ . Considering the thrust loading as concentrated at some non-dimensional position,  $x$ , along the blade span, then  $x$  will be the lever arm of the thrust moment.

Define a blade thrust moment coefficient as

$$C_{M_T} = \frac{M_T}{\rho \pi \Omega^2 R^5} \quad (35)$$

Thus, in non-dimensional form, the rotor blade thrust moment described above which acts instantaneously on a blade at some azimuth position,  $\psi$ , becomes

$$\int_{x_1}^{x_2} \frac{dC_{M_T}}{dx} dx = \int_{x_1}^{x_2} \frac{dC_T}{dx} x dx \quad (36)$$

where  $dC_T/dx$  is given in Equation (30).

To get the average value of the thrust moment acting on a rotor blade, consider one complete revolution of a blade and integrate Equation (36) from  $\psi = 0$  to  $\psi = 2\pi$ . Thus

$$C_{MT} = \left( \frac{1}{2\pi} \right) \int_0^{2\pi} \left[ \int_{x_1}^{x_2} \frac{dC_T}{dx} x dx \right] d\psi \quad (37)$$

However, inspection of Equation (37) reveals that the bracketed term is nearly the same as that given in Equation (25), which was expanded as Equation (31). The  $x$  multiplier in Equation (37) is the only difference. The  $x$  multiplier has the simple effect of increasing  $x^{n-1}$  to  $x^n$  in all integral multipliers of Equation (31). The integral multipliers are given by Equation (32). Further consideration of Equation (32) shows that increasing  $x^{n-1}$  to  $x^n$  is the same as increasing  $\bar{\theta}_n$  to  $\bar{\theta}_{n+1}$ .

Thus, increasing the integral multipliers in Equation (31) by one unit, substituting the result into Equation (37), and integrating with respect to  $\psi$  while noting the simplification afforded in Equation (34), the average rotor blade thrust moment is obtained as

$$\begin{aligned} C_{MT} = \frac{a\sigma}{2b} & \left[ \left( \lambda \mu^4 - \frac{1}{2} a_1 \mu^5 \right) \bar{\theta}_2 + \left( \frac{3}{2} A_0 \mu^4 + \frac{3}{16} a_1 \mu^3 - \frac{1}{4} \lambda \mu^2 \right) \bar{\theta}_3 \right. \\ & + \left( 2 \lambda \mu^2 - \frac{3}{2} a_1 \mu^3 + \frac{3}{2} \theta_1 \mu^4 - \frac{1}{4} A_0 \mu^2 \right) \bar{\theta}_4 + \left( \frac{5}{2} A_0 \mu^2 - \frac{1}{4} \theta_1 \mu^2 \right) \bar{\theta}_5 \\ & \left. + \left( \lambda + \frac{5}{2} \theta_1 \mu^2 - a_1 \mu \right) \bar{\theta}_6 + (A_0) \bar{\theta}_7 + (\theta_1) \bar{\theta}_8 \right] \quad (38) \end{aligned}$$

Rotor Rolling Moment.--From Fig. 4 it can be seen that the thrust moment of an element of thrust located at non-dimensional radius  $x$  has an in-



stantaneous moment arm  $x \sin \psi$  about the x-axis. Defining the x-axis as the rotor rolling axis, the resulting moment described above is termed the rotor rolling moment,  $M_X$ .

Define a rotor rolling moment coefficient as

$$C_{MX} = \frac{M_X}{\rho \pi \Omega^2 R^5} \quad (39)$$

Thus, in non-dimensional form, the rotor blade rolling moment which acts instantaneously on a blade at some azimuth position,  $\psi$ , becomes

$$\int_{x_1}^{x_2} \frac{dC_{MX}}{dx} dx = \int_{x_1}^{x_2} \frac{dC_T}{dx} x \sin \psi dx \quad (40)$$

To get the average value of the rotor rolling moment per revolution, follow the same procedure discussed between Equations (36) and (38). However, in this case, the multiplier on  $dC_T/dx$  is  $x \sin \psi$  instead of  $x$ . This gives no trouble, since the simplification afforded by Equation (34) still applies. Furthermore, note that

$$\frac{1}{2\pi} \int_0^{2\pi} \sin^2 \psi d\psi = \frac{1}{2} \quad (41)$$

Thus, the average value of the rotor rolling moment for a rotor with  $b$  blades becomes

$$C_{MX} = \frac{a\sigma}{4} \left[ (A_0 \mu^5) \bar{\delta}_2 + (\lambda \mu^3 - \frac{3}{8} A_0 \mu^3 + \theta \mu^5 - \frac{7}{4} a_1 \mu^4) \bar{\delta}_3 + (3A_0 \mu^3 \right.$$

$$\begin{aligned}
& + \frac{3}{8} a_1 \mu^2 - \frac{3}{8} \theta_1 \mu^3) \bar{a}_4 + (\lambda \mu + 3 \theta_1 \mu^3 - \frac{11}{4} a_1 \mu^2) \bar{a}_5 + (2A_0 \mu) \bar{a}_6 \\
& + (2 \theta_1 \mu - a_1) \bar{a}_7 \Big] \tag{42}
\end{aligned}$$

Rotor Pitching Moment.--From Fig. 4 it can be seen that the thrust moment of an element of thrust located at non-dimensional radius  $x$  has an instantaneous moment arm  $x \cos \psi$  about the y-axis. Defining the y-axis as the rotor pitching axis, the resulting moment described above is termed the rotor pitching moment,  $M_Y$ .

Define a rotor pitching moment coefficient as

$$C_{MY} = \frac{M_Y}{\rho \pi \Omega^2 R^5} \tag{43}$$

Thus, in non-dimensional form, the rotor blade pitching moment which acts instantaneously on a blade at some azimuth position,  $\psi$ , becomes

$$\int_{x_1}^{x_2} \frac{dC_{MY}}{dx} dx = \int_{x_1}^{x_2} \frac{dC_T}{dx} x \cos \psi dx \tag{44}$$

To get the average value of the rotor pitching moment per revolution, follow the same procedure discussed between Equations (36) and (38). However, in this case, the multiplier on  $dC_T/dx$  is  $x \cos \psi$  instead of  $x$ . This gives no trouble, since the simplification afforded by Equation (34) still applies. Furthermore, note that

$$\frac{1}{2\pi} \int_0^{2\pi} \cos^2 \psi d\psi = \frac{1}{2} \tag{45}$$

Thus, the average value of the rotor pitching moment for a rotor with  $b$  blades becomes

$$C_{MY} = \frac{a_0 \sigma}{4} \left[ (-a_0 \mu^5) \bar{\delta}_2 + \left( \frac{5}{4} b_1 \mu^4 + \frac{1}{8} a_0 \mu^3 \right) \bar{\delta}_3 + \left( -2a_0 \mu^3 - \frac{1}{8} b_1 \mu^2 \right) \bar{\delta}_4 + \left( \frac{9}{4} b_1 \mu^2 \right) \bar{\delta}_5 + (-a_0 \mu) \bar{\delta}_6 + (b_1) \bar{\delta}_7 \right] \quad (46)$$

In summary, Equations (33), (38), (42), and (46) give four equations with which to solve for the four unknown rotor parameters  $a_0$ ,  $A_0$ ,  $a_1$ , and  $b_1$ . This will be done in the next section.

Equilibrium Solution for Rotor Parameters.--Consider a centrally hinged, freely-flapping rotor system. For equilibrium steady state flight

$C_{MX} = 0$ . Furthermore, if it is assumed that rotor forces are in equilibrium and that there is no work done by the motion along the flight path of unbalanced residual forces, then Equations (33) and (42) can be solved simultaneously for  $A_0$  and  $a_1$ . Thus,

$$a_1 = \frac{(ZS - YN)}{(XS - MY)} \quad (47)$$

$$A_0 = \frac{(MZS - NYM - NZS - N^2 Y)}{(XS^2 - MYS)} \quad (48)$$

where the equilibrium factors  $X$ ,  $Y$ ,  $Z$ ,  $M$ ,  $N$  and  $S$  are all independent of  $a_0$ ,  $A_0$ ,  $a_1$ ,  $b_1$ , and may be found in the Appendix. It was convenient to solve for  $a_1$  and  $A_0$  (independent of  $a_0$  and  $b_1$ ) first, since the following equation for  $a_0$  will contain  $a_1$ ,  $A_0$ , and be independent of  $b_1$ .



The steady part of the blade inertia moment about the flapping hinge is largely the centrifugal moment since second and higher harmonic flapping, with respect to the tip-path plane, have been neglected. The centrifugal moment, from Reference 2, is given by  $a_o I_1 \Omega^2$  where  $I_1$  is the blade mass moment of inertia about the flapping hinge. Thus, for equilibrium, the thrust moment must balance the centrifugal moment about the flapping hinge as

$$M_T \approx a_o I_1 \Omega^2 \quad (49)$$

or non-dimensionally

$$C_{MT} = \frac{a_o I_1 \Omega^2}{\rho \pi R^5} = a_o \left[ \frac{I_1}{\rho \pi R^5} \right] \quad (50)$$

Thus, substituting Equation (38) into (50) and solving for  $a_o$  gives

$$\begin{aligned} a_o = K \left[ \left( \lambda \mu^4 - \frac{1}{2} a_1 \mu^5 \right) \bar{a}_2 + \left( \frac{3}{2} A_o \mu^4 + \frac{3}{16} a_1 \mu^3 - \frac{1}{4} \lambda \mu^2 \right) \bar{a}_3 + \left( 2 \lambda \mu^2 \right. \right. \\ \left. \left. - \frac{3}{2} \theta_1 \mu^4 - \frac{1}{4} A_o \mu^2 \right) \bar{a}_4 + \left( \frac{5}{2} A_o \mu^2 - \frac{1}{4} \theta_1 \mu^2 \right) \bar{a}_5 + \left( \lambda + \frac{5}{2} \theta_1 \mu^2 \right. \right. \\ \left. \left. - a_1 \mu \right) \bar{a}_6 + (A_o) \bar{a}_7 + (\theta_1) \bar{a}_8 \right] \quad (51) \end{aligned}$$

where  $K = \left[ \frac{\rho \pi R^5 \sigma a}{2b I_1} \right]$  rotor blade inertia factor.

Also, considering equilibrium steady state flight,  $C_{MY} = 0$ .

Thus, setting Equation (46) equal to zero and solving for  $b_1$  gives

$$b_1 = \frac{1}{\left[ -\bar{\delta}_7 + \frac{1}{8}\mu^2\bar{\delta}_4 - \frac{5}{4}\mu^4\bar{\delta}_3 - \frac{9}{4}\mu^2\bar{\delta}_2 \right]} \left[ (-a_o\mu^5)\bar{\delta}_2 + \left( \frac{1}{8}a_o\mu^3\bar{\delta}_3 + (-2a_o\mu^3)\bar{\delta}_4 + (-a_o\mu)\bar{\delta}_6 \right) \right] \quad (52)$$

Note that  $b_1$  is only a function of  $a_o$ , and that  $a_o$  is obtained from Equation (51) which, in turn, is evaluated from Equations (47) and (48). Thus, a convenient sequence has been established for evaluating  $a_1$ ,  $A_o$ ,  $a_o$ , and then  $b_1$ .

Equations (47), (48), (51), and (52) take into account the effects of the radial component and are needed to evaluate the preceding rotor thrust and moment expressions. They will also be needed to solve the helicopter power required expressions, which will be derived in the next section. In evaluating Equations (47), (48), (51), and (52) it should be remembered that the integral multipliers,  $\bar{\delta}_n = 1, 2, 3, 4, \dots$ , are given in Table I.

Rotor Lift Power.--In this section an equation including the effects of  $v_r$  and representing that part of the total helicopter power required due to blade lift forces will be derived. The power required for the lift on a blade element is equal to the component of lift multiplied by its associated velocity component. Thus, the differential lift power required as seen from Fig. 3 is

$$(dP)_{RL} = (dL)_t (\Omega R v_t) \quad (53)$$

where  $\Omega R$  dimensionalizes  $v_t$ . However, Equation (53) cannot be conveniently integrated, and must be expressed in another form. From the

conservation of energy, the energy per unit time input to the blade,  $(dL)_t (\Omega R v_t)$ , is equivalent to the energy output by the blade,  $(dL)_a (\Omega R v_a)$ . With this in mind Equation (53) may be re-written as

$$(dP)_{RL} = - (dL)_a (\Omega R v_a) \quad (54)$$

in which the minus sign is placed since  $(dP)_{RL}$  must be positive when there is a downflow through the rotor represented by a negative  $v_a$ .

Substituting Equation (18) into (54) gives

$$(dP)_{RL} = - \rho \Omega^2 R^2 \Gamma v_a v_t dr \quad (55)$$

Substituting Equation (16) into (55) gives

$$(dP)_{RL} = - \frac{\rho a c \Omega^3 R^5}{2} v_a (\theta v_t + v_a) \sqrt{v_t^2 + v_r^2} dr \quad (56)$$

Define a non-dimensional power coefficient as

$$C_P = \frac{P}{\rho \pi \Omega^3 R^5} \quad (57)$$

Finally, substituting Equations (27), (29), and (57) into (56), while noting that  $\frac{dr}{R} = dx$ , gives

$$\frac{(dC_P)_{RL}}{dx} = - \frac{a c}{2 \pi R} v_a (\theta v_t + v_a) (x^2 + \mu^2)^{1/2} (1 + F - \frac{1}{2} F^2) \quad (58)$$

which represents the lift power loading required due to the variation in spanwise inflow angle and lift.

However, it is desired to obtain an expression for the average lift

power required of the whole rotor for any flight condition. This is found by integrating Equation (58) from a blade inboard section,  $x_1$ , to some outboard section,  $x_2$ , and then taking the average value for the revolution by integrating azimuthally from  $\psi = 0$  to  $\psi = 2\pi$ . Multiplying by the  $b$  number of blades in the rotor system gives the desired result. Then

$$C_{PRL} = \frac{a\sigma}{2} \left( \frac{1}{2\pi} \right) \int_0^{2\pi} \int_{x_1}^{x_2} v_a (\theta v_t + v_a) (x^2 + \mu^2)^{1/2} (1 + F - \frac{1}{2} F^2) dx d\psi \quad (59)$$

To carry out the integration indicated in Equation (59) substitute Equations (4), (5), (7), and (28) into the integrand, expand the result, and integrate term by term. The same simplification afforded by Equation (34) applies and the integral multipliers are given by Equation (32). The result is written in the following tabular form (Equation (60)) where the coefficients in the boxes must each be multiplied by its corresponding row and column head. After summing all individual products of a boxed coefficient, its row head, and its column head, the resulting lengthy expression represents the average value of  $C_{PRL}$  per revolution.



$$\frac{4C_{PRL}}{a_0} =$$

	1	$\mu$	$\mu^2$	$\mu^3$	$\mu^4$	$\mu^5$	$\mu^6$
$\bar{\alpha}_1$					$-2\lambda^2$	$a_1\lambda$	$-a_0^2$
$\bar{\alpha}_2$			$\frac{1}{2}\lambda^2$	$-\frac{3}{8}a_1\lambda$	$-3A_0\lambda + \frac{1}{8}a_0^2$	$-b_1a_0$	$\frac{1}{4}b_1a_0$
$\bar{\alpha}_3$			$-4\lambda^2 + \frac{1}{2}A_0\lambda + \frac{1}{2}\theta_1\lambda$	$2a_1\lambda - \frac{1}{8}b_1a_0$	$-2\theta_1\lambda - 2a_0^2$	$-\theta_1\lambda$	
$\bar{\alpha}_4$			$-5A_0\lambda$	$\frac{7}{4}b_1a_0$			
$\bar{\alpha}_5$	$-2\lambda^2$	$2a_1\lambda$	$-5\theta_1\lambda - a_0^2$				
$\bar{\alpha}_6$	$-2A_0\lambda$	$b_1a_0$					
$\bar{\alpha}_7$	$-2\theta_1\lambda$						

(60)

Rotor Profile Power.--It is now desired to derive an expression for the rotor profile power required, taking into account the effects of the radial velocity component. In the non-viscous, ideal fluid the only power was that required to overcome rotor blade lift forces. In an incompressible viscous fluid, additional power must be applied to the rotor in order to overcome skin friction and pressure drag forces. However, the usual subsonic operation below the stall will be assumed. Under this conventional

assumption the viscous resistance to blade motion is mostly due to fluid shearing forces in laminar and turbulent boundary layers (defined as skin friction drag).

Hence, the differential profile drag force,  $dD$ , acting on the differential blade element,  $cdr$ , at radius,  $r$ , and azimuth position,  $\psi$ , and acting in the direction of the resultant velocity,  $U$ , is in large part skin friction and is written

$$dD = C_{do} \frac{1}{2} \rho U^2 cdr \quad (61)$$

where  $U$  is given in Equation (8).

Equation (61) may be split into three components by writing  $U^2$  as  $U(U)$  and substituting for  $U$  in parenthesis its value from Equation (8). Thus, for the axial component of Equation (61) set  $v_r = v_t = 0$ . The result is

$$(dD)_a = C_{do} \frac{1}{2} \rho U(\Omega R v_a) cdr \quad (62)$$

Likewise, radial and tangential components become respectively

$$(dD)_r = C_{do} \frac{1}{2} \rho U(\Omega R v_r) cdr \quad (63)$$

$$(dD)_t = C_{do} \frac{1}{2} \rho U(\Omega R v_t) cdr \quad (64)$$

Thus, the energy per second or the differential profile power dissipated at the blade element  $cdr$  due to component skin friction drag forces may be expressed by the relation

$$(dP)_{RD} = \left( \sqrt{(dD)_2^2 + (dD)_t^2 + (dD)_r^2} \right) U \, dr \quad (65)$$

Substituting Equations (62), (63), and (64) into (65) then yields

$$(dP)_{RD} = \frac{1}{2} \rho U \Omega^2 R^2 c_{do} (v_a^2 + v_t^2 + v_r^2) dr \quad (66)$$

Equation (66) still leaves much to be desired, since it cannot be conveniently integrated as it stands. Further development of the terms  $U$  and  $C_{do}$  must be made.

Following essentially the same procedure in the series approximation of Equation (27), the term,  $U$ , of Equation (66), contains the troublesome radical,  $\sqrt{v_a^2 + v_t^2 + v_r^2}$ , which may be expanded by the binomial theorem. Then, since  $a_o$  is small for conventional designs, the resulting expansion from Reference 1 becomes

$$\frac{U}{\Omega R} = \sqrt{x^2 + \mu^2 + \lambda^2} \left( 1 + G - \frac{1}{2} G^2 \right) \quad (67)$$

where

$$G \approx \frac{\mu x \sin \psi}{x^2 + \mu^2 + \lambda^2} \quad (68)$$

and Equation (67) is in non-dimensional form. For  $\lambda \neq 0$  the series in Equation (67) converges for all values of  $\mu$ ,  $x$ ,  $\psi$  and  $\lambda$ . Castles, in Reference 1, explains that the convergence is similar to, but somewhat more rapid than, that of Equation (27), and will give accurate results when incorporated into the profile power expression.

The local blade profile drag coefficient,  $C_{do}$ , will now be con-

sidered. Payne, in Reference 4, explains that for smooth, thin airfoils in incompressible, viscous flow operating at subsonic speeds below the stall, the blade element profile drag is essentially skin friction and is given by the non-dimensional relation

$$C_{do} = 2 C_f (1 + C_l^2) \quad (69)$$

where  $C_f$  is an average skin friction drag coefficient which, for smooth surfaces and the usual Reynolds Numbers (i.e.,  $1.0 \times 10^6$  to  $4.0 \times 10^6$ ), is of the order  $C_f \approx 0.004$ , as seen in Reference 4.

To relate Equation (69) to the case at hand, first, Equation (15) is re-written

$$C_l = \frac{2\Gamma}{cU} \quad (70)$$

Substituting Equations (8), (11), and (16) into (70) yields

$$C_l = \frac{a(\theta v_t + v_a)}{\sqrt{v_a^2 + v_t^2 + v_r^2}} \quad (71)$$

With the expressions for  $U$  and  $C_{do}$  thus obtained, Equation (66) can be put into integrable form. Hence, substituting Equations (67), (69), and (71) into (66), non-dimensionalizing with Equation (57), and remembering that  $dr = Rdx$ , the result is

$$\frac{(dC_P)_{RD}}{dx} = \frac{cC_f}{\pi R} \left[ (v_a^2 + v_t^2 + v_r^2) + a^2(\theta v_t + v_a)^2 \right] \cdot (x^2 + u^2 + \lambda^2)^{1/2} \left( 1 + G - \frac{1}{2} G^2 \right) \quad (72)$$



which gives the spanwise differential profile power loading required to mainly overcome skin friction. Note that  $v_r$  is included in Equation (72).

However, it is desired to obtain an expression for the average profile power required of the whole rotor for any flight condition. This is found by integrating Equation (72) from a blade inboard section,  $x_1$ , to some outboard section,  $x_2$ , and then taking the average value for the revolution by integrating azimuthally from  $\psi = 0$  to  $\psi = 2$ . Multiplying the result by the  $b$  number of blades in the rotor system gives the desired result. Thus

$$C_{PRD} = \sigma C_f \left( \frac{1}{2\pi} \right) \int_0^2 \int_{x_1}^{x_2} \left[ (v_a^2 + v_t^2 + v_r^2) + a^2 (\theta v_t + v_a)^2 \right] \cdot \\ \cdot (x^2 + \mu^2 + \lambda^2)^{1/2} \left( 1 + G - \frac{1}{2} G^2 \right) dx d\psi \quad (73)$$

To carry out the integration indicated in Equation (73), substitute Equations (4), (5), (6), (7), and (68) into the integrand, expand the result, and integrate term by term. The same simplification afforded by Equation (34) applies and the integral multipliers are given by

$$\mathfrak{I}'_n = \int_{x_1}^{x_2} \frac{x^{n-1} dx}{\left[ x^2 + (\mu^2 + \lambda^2) \right]^{3/2}} \quad (74)$$

where for high speed forward flight  $\mu^2 \gg \lambda^2$ . Hence, as a first approximation  $\lambda^2$  can be dropped from Equation (74). With the previous assumption Equation (74) becomes identical to Equation (32) (i.e.,  $\bar{\alpha}_n \equiv \bar{\alpha}'_n$ ). Thus, Table I may be used in evaluating  $C_{PRD}$ .

The result of the integration in Equation (73) is written for convenience in the following tabular form (Equation (75)) where the coefficients in the boxes must each be multiplied by its corresponding row and column head. After summing all individual products of a boxed coefficient, its row head, and its column head, the resulting lengthy expression represents the average value of  $C_{PRD}$  per revolution.

$$\frac{2 C_{PRD}}{a^2 \sigma C_f} =$$

	1	$\mu$	$\mu^2$	$\mu^3$	$\mu^4$	$\mu^5$	$\mu^6$
$\pi'_1$	$\frac{2\lambda^6}{a^2} + \frac{\lambda^4 a_o^2}{a^2}$	$-2a_1\lambda^5 + a_o\lambda^4$	$\frac{6\lambda^4}{a^2} + A_o^2\lambda^4 + \frac{3}{4}a_1^2\lambda^4 + \frac{2a_o^2}{a^2}$	$2a_o^2\lambda^2 - 4a_1\lambda^3$	$\frac{6\lambda^2}{a^2} + 2A_o\lambda^2 + a_1^2\lambda^2 + \frac{a_o^2}{a^2}$	$-2\lambda a_1$	$\frac{2}{a^2} + A_o^2 + \frac{3}{4}a_1^2 + a_o^2$
$\pi'_2$	$2A_o^2\lambda^4 + 4A_o\lambda^5$	$2a_1^2\lambda^4 - 4A_o a_1\lambda^4 + 2b_1 a_o\lambda^4$	$2A_o\theta_1\lambda^4 + 4A_o^2\lambda^2 + 10A_o\lambda^3$	$4a_1^2\lambda^2 - \frac{19}{2}A_o a_1\lambda^2 - \frac{9}{2}b_1 a_o\lambda^2$	$2A_o^2 + 6A_o\lambda + 4A_o\theta_1\lambda^2$	$2a_1^2 - \frac{11}{2}A_o a_1 - \frac{5}{2}b_1 a_o$	$2A_o\theta_1$
$\pi'_3$	$\frac{6\lambda^4}{a^2} + 4\theta_1\lambda^5 + a_1^2\lambda^4 + b_1^2\lambda^4 + \frac{2\lambda^2 a_o^2}{a^2}$	$-2\theta_1 a_1\lambda^2 - 6\lambda^3 a_1 - 4\theta_1 a_1\lambda^4$	$\frac{27}{2a^2} + \frac{17a_o^2}{8a^2} \frac{1}{2}\lambda^2 + 4A_o^2\lambda^2 + \frac{11}{4}a_1^2\lambda^2 + 2a_o^2 + \theta_1^2\lambda^4 + 10\theta_1\lambda^3 + \frac{5}{2}b_1^2\lambda^3$	$-2\theta_1 a_1 - \frac{21}{4}\lambda a_1 - \frac{19}{2}\theta_1 a_1\lambda^2$	$\frac{15}{2a^2} + \frac{29}{8}A_o^2 + \frac{23}{16}a_1^2 + 2a_o^2 \frac{1}{8} + 6\theta_1\lambda + \frac{23}{16}b_1^2 + 2\theta_1^2\lambda^2$	$-\frac{11}{2}\theta_1 a_1$	$\theta_1^2$
$\pi'_4$	$4A_o^2\lambda^2 + 8A_o\lambda^3 + 4A_o\theta_1\lambda^4$	$4a_1^2\lambda^2 - 10A_o a_1\lambda^2 - 4b_1 a_o\lambda^2$	$4A_o^2 + 9A_o\lambda + 16A_o\theta_1\lambda^2$	$\frac{13}{4}a_1^2 - \frac{23}{2}A_o a_1 - \frac{19}{4}b_1 a_o$	$\frac{45}{4}A_o\theta_1$		

(continued)

(75)

	1	$\mu$	$\mu^2$	$\mu^3$	$\mu^4$	$\mu^5$	$\mu^6$
$\Phi'_5$	$\frac{6\lambda^2}{a^2} + 8\theta_1\lambda^3$ $+ 2a_1\lambda^2 + 2b_1^2\lambda^2$ $+ 2\theta_1^2\lambda^4 + \frac{a_0^2}{a^2}$	$-4\lambda a_1 - 6a_1\theta_1\lambda^2$	$\frac{15}{2a^2} + \frac{5A_0^2}{2a_0^2} + a_0^2$ $+ 9\theta_1\lambda + 2a_1$ $+ \frac{19}{8}b_1^2 + 8\theta_1^2\lambda^2$	$- 6\theta_1 a_1$	$\frac{45}{8}\theta_1^2$		
$\Phi'_6$	$4A_0\lambda + 8A_0\theta_1\lambda^2$	$2a_1^2 - 6A_0a_1$ $- 2b_1a_0$	$13 A_0\theta_1$				
$\Phi'_7$	$\frac{2}{a^2} + 2A_0^2 + 4\theta_1\lambda$ $+ a_1^2 + b_1^2 + 4\theta_1^2\lambda^2$	$- 6\theta_1 a_1$	$6\theta_1^2$				
$\Phi'_8$	$4 A_0\theta_1$						
$\Phi'_9$	$2\theta_1^2$						

(concluded)

(75)

Total Helicopter Power Required.--The last step in this analysis is to develop an equation for the total helicopter power required which incorporates the effects of the radial velocity component. The complete expression is constructed by combining Equations (60) and (75), since total helicopter power required is equal to the lift power plus the profile power. Thus, in non-dimensional form, the equation would be

$$C_{PRT} = \frac{a\sigma}{4} \sum_{i=0}^{i=6} \sum_{n=1}^{n=7} C_{in} \mu^i \bar{a}_n + \frac{a^2 \sigma C_f}{2} \sum_{i=0}^{i=6} \sum_{n=1}^{n=9} C_{in} \mu^i \bar{a}'_n$$

$$= C_{PRL} + C_{PRD} \quad (76)$$

where the summations represent the expansion of the tabular forms of Equations (60) and (75). That is, each boxed term,  $C_{in}$ , in the  $i$ -th column and the  $n$ -th row is to be multiplied by its corresponding  $i$ -th column head,  $\mu^i$ , its  $n$ -th row head,  $\bar{a}_n$  or  $\bar{a}'_n$ ; then all individual products are summed.

Inspection of Equations (60) and (75) will show that Equation (76) is quite lengthy. Furthermore, Equation (76) would have to be modified for compressibility and rotor blade stall under the most general assumptions of this analysis.

However, a useful expression can be obtained for  $C_{PRT}$  for speeds below that at which tip stall on the retreating blade occurs. Thus, the following order analysis is performed.

Assume that terms containing powers of  $\mu$  higher than the fourth are small and can be dropped. Next, consider fifth and higher order products of  $\mu$ ,  $\lambda$  and the blade angles are small and can be dropped.



Lastly, drop all terms containing  $a_0$  and  $b_1$  since experience shows that such terms tend to cancel one another. Thus, the result of expanding Equation (76) becomes

$$\begin{aligned}
 C_{PRT} = & \frac{a\sigma}{4} \left[ \left( \frac{1}{2} \lambda^2 \mu^2 \right) \bar{\delta}_2 + \left( \frac{1}{2} A_0 \lambda \mu^2 - 4 \lambda^2 \mu^2 + \frac{1}{2} \theta_1 \lambda \mu^2 \right) \bar{\delta}_3 \right. \\
 & + \left( -5 A_0 \lambda \mu^2 \right) \bar{\delta}_4 + \left( -2 \lambda^2 + 2 a_1 \lambda \mu - 5 \theta_1 \lambda \mu^2 \right) \bar{\delta}_5 \\
 & \left. + \left( -2 A_0 \lambda \right) \bar{\delta}_6 + \left( -2 \theta_1 \lambda \right) \bar{\delta}_7 \right] + \frac{a^2 \sigma C_f}{2} \left[ \left( \frac{6 \lambda^4}{a^2} + \frac{27}{2a^2} \mu^2 \right. \right. \\
 & - \frac{1}{2} \lambda^2 \mu^2 + \frac{15}{2a^2} \mu^4 - \frac{1}{8} \mu^4 \right) \bar{\delta}'_3 + \left( 4 A_0^2 \lambda^2 + 8 A_0 \lambda^3 + 4 A_0^2 \mu^2 \right. \\
 & + 9 A_0 \lambda \mu^2 \right) \bar{\delta}'_4 + \left( \frac{6 \lambda^2}{a^2} + 8 \theta_1 \lambda^3 + 2 a_1 \lambda^2 - 4 \lambda a_1 \mu + \frac{15}{2a^2} \mu^2 \right. \\
 & + \frac{5}{2} A_0^2 \mu^2 + 9 \theta_1 \lambda \mu^2 + 2 a_1 \mu^2 \right) \bar{\delta}'_5 + \left( 4 A_0 \lambda + 8 A_0 \theta_1 \lambda^2 + 2 a_1^2 \mu \right. \\
 & - 6 A_0 a_1 \mu + 13 A_0 \theta_1 \mu^2 \right) \bar{\delta}'_6 + \left( \frac{2}{a^2} + 2 A_0^2 + 4 \theta_1 \lambda + a_1^2 + 4 \theta_1^2 \lambda^2 \right. \\
 & \left. \left. - 6 \theta_1 a_1 \mu + 6 \theta_1^2 \mu^2 \right) \bar{\delta}'_7 + \left( 4 A_0 \theta_1 \right) \bar{\delta}'_8 + \left( 2 \theta_1^2 \right) \bar{\delta}'_9 \right] \quad (77)
 \end{aligned}$$

Since Equation (77) is approximate, it is convenient to assume that

$\bar{\delta}_n \approx \bar{\delta}'_n$ . Thus, Table I can be used to facilitate the evaluation of Equation (77). The unknowns,  $A_0$  and  $a_1$ , are obtained from Equations (47) and (48), respectively.

To complete a tip-path plane analysis an equation for the rotor X-force must be included. Such an equation is obtained from Reference 2 and is given in the Appendix.

## CHAPTER III

## APPLICATION

Sample Problem.--It is desired to compare two computed values of the power required for a given flight condition. The first value computed using Equation (77) (which accounts for  $v_r$ ) will be compared with a similar value computed using the equation in the Appendix (which neglects  $v_r$ ). The helicopter considered will be the Bell YHU-1B and the following given data were obtained from Reference 5.

Given Data:

$$V = 193 \text{ mph}$$

$$b = 2$$

$$f = 20 \text{ ft}^2$$

$$\theta_1 = 10^\circ$$

$$W = 6000 \text{ lbs}$$

$$a_0 = 4^\circ$$

$$\sigma = 0.051$$

$$\Omega = 323 \text{ rpm}$$

$$R = 22 \text{ ft}$$

Approximate Procedure: Where not specifically stated, terms used in the following procedure are defined in the List of Symbols.

- 1) Assume that  $T = W$  as a first approximation in calculating  $C_T$ .
- 2) As a first approximation neglect  $F_x$  and compute  $\alpha_R$  from  $\alpha_R \approx \tan^{-1} D_F/W$ .
- 3) Use Equations (47) and (48) in calculating  $a_1$  and  $A_0$  to be used in Equation (77).
- 4) Since Equation (77) is based on a uniform induced velocity,  $v_i$ , use the expression for  $\lambda$  obtained from Reference 6.

- 5) The equation for  $C_{PR}$  in the Appendix is based on a triangular induced velocity,  $v_i$ . Thus, use the theory of Reference 2 to compute  $v_i$ .
- 6) As a first approximation assume  $\lambda \approx 0$  in the integral multipliers given by Equation (74). Thus, Equation (74) becomes identical to Equation (32) (i.e.,  $\bar{a}_n \equiv \bar{a}'_n$ ). Thus, for the corresponding  $\mu$  at  $V = 193$  mph interpolate values for the  $\bar{a}_n$ 's from Fig. 5.
- 7) Values obtained above are included in Table II, from which the equations for  $C_{PRT}$  and  $C_{PR}$  are evaluated.
- 8) Neglect transmission and tail rotor losses.

Approximate Results: From the evaluation of Equations (77) for  $C_{PRT}$  and the equation for  $C_{PR}$  in the Appendix, it was found, dimensionally, that for the given flight condition the total power required became

(with $v_r$ )	$P_R = 1550$ shp
(without $v_r$ )	$P_R = 1290$ shp

where it was found that

$$C_{PRL} = 0.000456$$

$$C_{PRD} = 0.000120$$

## CHAPTER IV

### CONCLUSIONS

Force, moment, and power equations, including the effects of the radial component of the resultant velocity at the rotor blade elements, were derived. Integral multipliers contained in the derived equations were tabulated. With data obtained on the Bell YHU-1B, the power required was calculated at a high forward speed flight condition, both with the equations derived and similar ones neglecting the radial velocity component. A resulting comparison shows that the effects of the radial component on the power required are as follows:

- 1) For the Bell YHU-1B the calculated total power required will be increased about 15 per cent when the effects of the radial velocity component at the blade elements are taken into account.
- 2) Of the total power required for the YHU-1B, that part due to lift will be increased about 10 per cent due to the effects of the radial velocity component.
- 3) Of the total power required for the YHU-1B, that part due to profile drag will be increased about 20 per cent due to the effects of the radial velocity component.
- 4) In general, it is concluded from this investigation that theoretical prediction of the helicopter power required will underestimate the actual power required at high forward speeds when the effects of the radial velocity component are neglected.



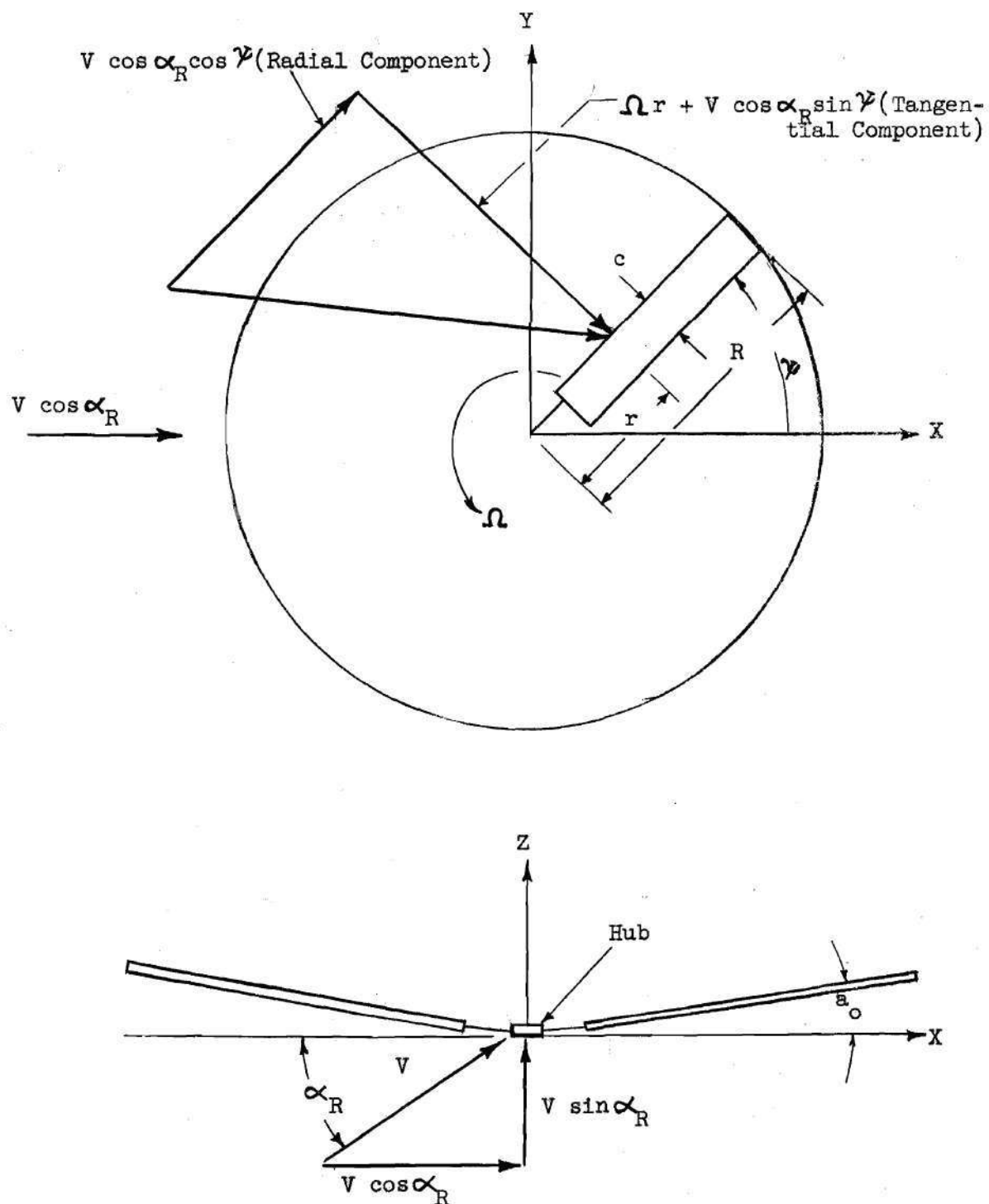


Fig. 1 Freestream and Relative Velocity Components in Rotor Tip-Path Plane Co-ordinate System (all velocities, lengths, and angles shown positive)



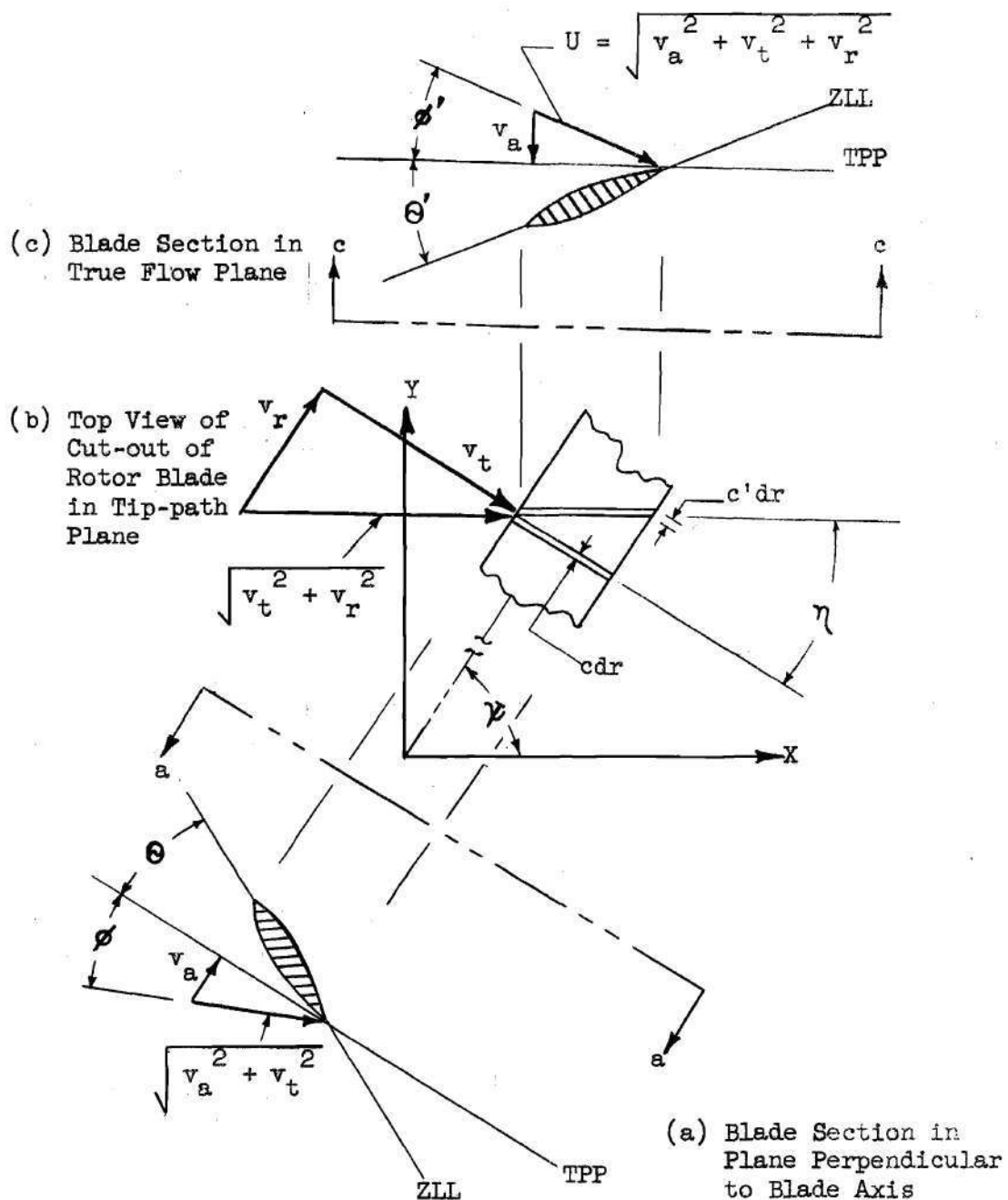


Fig. 2 Three View of Flow Planes, Velocity Components and Flow Angles (all shown positive)

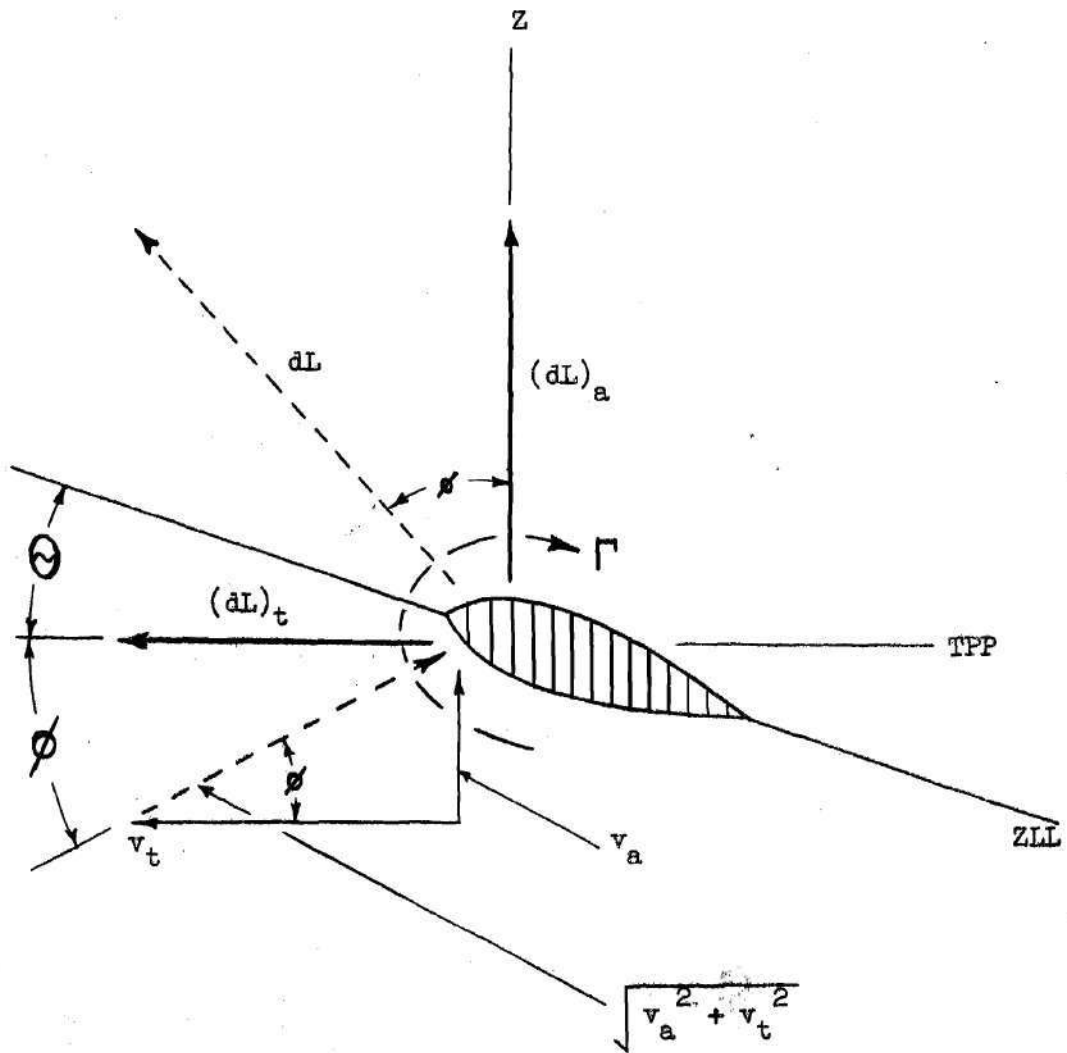


Fig. 3 Lift Force Components in Plane Perpendicular to Blade Axis

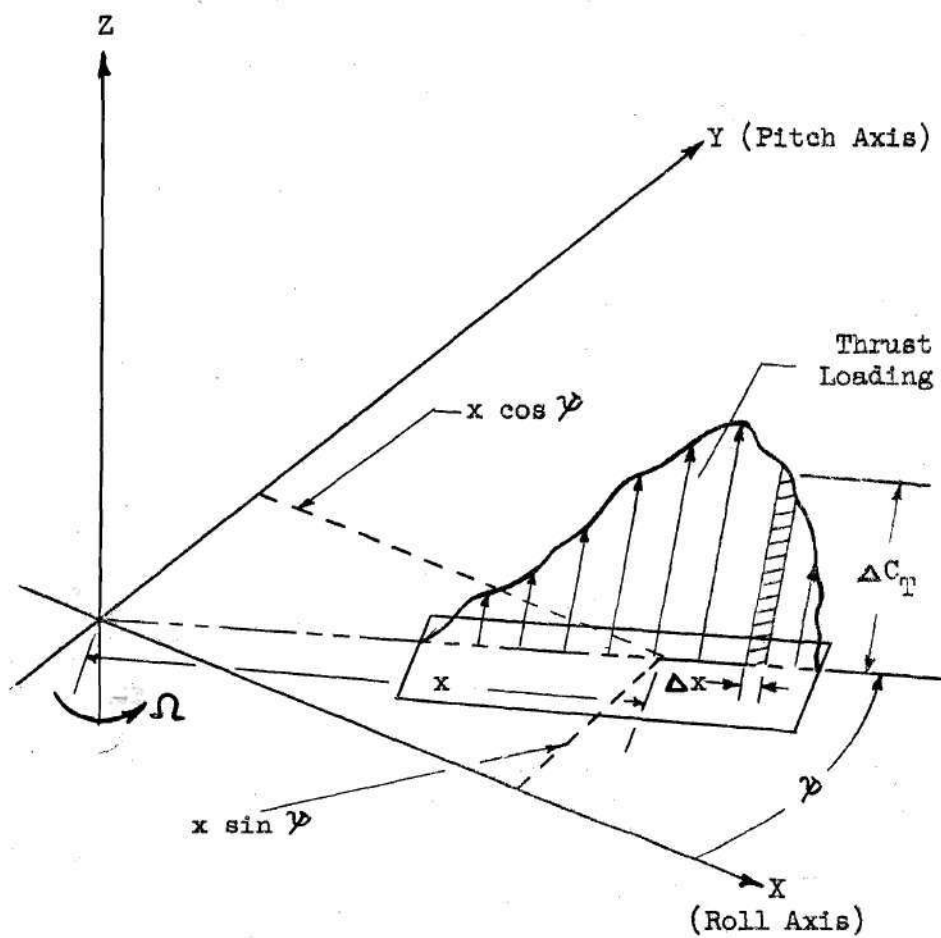


Fig. 4 Blade Loading and Moment Diagram

Table 1

## Integral Multipliers for Various Helicopter

## Forward Speed Ratios

$\mu$	$\bar{a}_1$	$\bar{a}_2$	$\bar{a}_3$	$\bar{a}_4$	$\bar{a}_5$	$\bar{a}_6$	$\bar{a}_7$	$\bar{a}_8$	$\bar{a}_9$
0.0	14.1020	5.2614	1.8476	0.8904	0.4820	0.3210	0.2381	0.1745	0.1401
0.1	10.0300	3.4460	1.4230	0.7170	0.4287	0.2906	0.2144	0.1672	0.1355
0.2	6.8070	2.2525	1.1280	0.6065	0.3788	0.2637	0.1975	0.1555	0.1267
0.3	4.4510	1.7880	0.8639	0.4938	0.3217	0.2299	0.1750	0.1392	0.1142
0.4	2.9820	1.2820	0.6605	0.3967	0.2674	0.1954	0.1509	0.1212	0.1001
0.5	2.0690	0.9406	0.5089	0.3176	0.2198	0.1635	0.1278	0.1035	0.0861
0.6	1.4830	0.7043	0.3961	0.2545	0.1798	0.1357	0.1071	0.0874	0.0730
0.7	1.0940	0.5376	0.3115	0.2047	0.1470	0.1121	0.0893	0.0733	0.0615
0.8	0.8264	0.4173	0.2475	0.1656	0.1204	0.0927	0.0743	0.0613	0.0516
0.9	0.6372	0.3289	0.1987	0.1348	0.0990	0.0768	0.0619	0.0512	0.0433
1.0	0.5001	0.2627	0.1611	0.1105	0.0819	0.0639	0.0517	0.0429	0.0364

Table 2

## Values Used in Example Problem

$\mu$	0.367
$v$ (fps)	284
$D_F$ (lbf)	1920
$\alpha_R(o)$	- 16.7
$v_A$	- 0.110
$v_i$	0.00680
$v$	0.00390
$\lambda$	- 0.114
$C_T$	0.00301
$\theta_1$ (radian)	- 0.174
$A_o$ (radian)	0.127
$a_1$ (radian)	0.118
$\delta_2$	1.434
$\delta_3$	0.721
$\delta_4$	0.326
$\delta_5$	0.284
$\delta_6$	0.206
$\delta_7$	0.158
$\delta_8$	0.127
$\delta_9$	0.104



## APPENDIX

Equilibrium Factors.--The following terms are found in Equations (47) and (48):

$$M = (\frac{3}{16} \mu^3 \bar{a}_3 - \frac{1}{2} \mu^5 \bar{a}_2 - \frac{3}{2} \mu^3 \bar{a}_4 - \mu \bar{a}_6)$$

$$N = (\lambda \mu^4 \bar{a}_2 - \frac{1}{4} \lambda \mu^2 \bar{a}_3 + 2 \lambda \mu^2 \bar{a}_4 + \frac{3}{2} \theta_1 \mu^4 \bar{a}_4 - \theta_1 \mu^2 \bar{a}_5 \\ + \lambda \bar{a}_6 + \frac{5}{2} \theta_1 \mu^2 \bar{a}_6 + \theta_1 \bar{a}_8 - \frac{2C_T}{a\sigma})$$

$$S = (\frac{1}{4} \mu^2 \bar{a}_3 - \bar{a}_6 - \frac{3}{2} \mu^4 \bar{a}_2 - \frac{5}{2} \mu^2 \bar{a}_4)$$

$$X = (\bar{a}_7 + \frac{7}{4} u^4 \bar{a}_3 - \frac{3}{8} u^2 \bar{a}_4 + \frac{11}{4} u^2 \bar{a}_5)$$

$$Y = (\mu^5 \bar{a}_2 - \frac{3}{8} \mu^3 \bar{a}_3 + 3 \mu^3 \bar{a}_4 + 2 \mu \bar{a}_6)$$

$$Z = (\lambda \mu^3 \bar{a}_3 + \theta_1 \mu^5 \bar{a}_3 - \frac{3}{8} \theta_1 \mu^3 \bar{a}_4 + \lambda \mu \bar{a}_5 + 3 \theta_1 \mu^3 \bar{a}_5 \\ + 2 \mu \theta_1 \bar{a}_7)$$

X-Force Equation.--The following equation was obtained from Reference 2. The significance of the X-force is that it is needed for an accurate determination of  $\alpha_R$ . The X-force is the downwind component of inplane blade element lift and profile forces. Non-dimensionally

$$C_x = (\frac{C_T}{1 - \mu^2})(2 v_A - \frac{10}{3} v_i) \mu + \frac{\delta_o \sigma \mu}{2} - \frac{16 \epsilon}{\sigma} (\frac{C_T}{1 - \mu^2})^2 \mu$$

where the above equation neglects effects of reversed flow and the radial velocity component; however, nearly all other assumptions of the preceding analysis apply. Thus, as a first approximation the above equation may be used along with the other equations in the analysis.

Power Equation.--For comparison purposes, as in the example problem, the following equation from Reference 2 is included. This equation is similar to Equation (77) with one exception; namely, the following equation neglects the effects of the radial velocity component and reversed flow.

$$\begin{aligned}
 C_{PR} = & \left( \frac{C_T}{1 - \mu^2} \right) \left[ \frac{3}{4} v_i (1 + \frac{4}{3} \mu^2) - v_A \right] - \frac{a \sigma v_A v_i}{48} - \frac{a \sigma a_o^2 \mu^2}{72} + \frac{1}{8} \delta_o \sigma (1 \\
 & + v_A^2 - \frac{4}{3} v_A v_i + \frac{1}{2} v_i^2 + \mu^2) + \frac{9}{2} \epsilon \frac{C_T^2 (1 + \frac{8}{9} \mu^2)}{\sigma (1 - \mu^2)} + \frac{a^2 \epsilon \sigma}{8} (\frac{1}{4} v_A^2 \\
 & + \frac{1}{9} a_o^2 \mu^2)
 \end{aligned}$$

where  $v_i$  is the triangular induced velocity coefficient.

## BIBLIOGRAPHY

1. Castles, Walter, Jr., A Procedure for Incorporating the "Swept Wing" or Radial Velocity Corrections in Closed Form Lifting Rotor Theory, Unpublished Class Notes, School of Aerospace Engineering, Georgia Institute of Technology, 1961.
2. Castles, Walter, Jr., Helicopter Performance Estimation, Unpublished Class Notes, School of Aerospace Engineering, Georgia Institute of Technology, 1960.
3. Von Mises, Richard, Theory of Flight, 1st ed., New York: McGraw-Hill, Inc., 1945, p. 179.
4. Payne, P. R., Helicopter Dynamics and Aerodynamics, 1st ed., New York: The Macmillan Co., 1959, pp. 12-18.
5. Westphal, J. F., and Balfe, P. J., YHU-1B Category I Performance, Stability and Control Tests, Air Force Flight Test Center Technical Report 61-39, July, 1961.
6. Gessow, A., and Meyers, G. C., Jr., Aerodynamics of the Helicopter, 1st ed., New York: The Macmillan Co., 1952, p. 221.